Monomer and Dimer Complexes of Coronene with Atomic Ions

Boguslav P. Pozniak and Robert C. Dunbar*

Contribution from the Chemistry Department, Case Western Reserve University, Cleveland, Ohio 44106

Received May 19, 1997[⊗]

Abstract: Formation of ML^+ and ML_2^+ complexes of coronene was investigated with 25 atomic ions (M^+) in the low-pressure gas-phase environment of the Fourier-transform ion cyclotron resonance (FT-ICR) ion trapping mass spectrometer. All of the atomic ions formed $M^+(Cor)$ except the alkalis (and also excepting a few cases which were dominated by charge transfer). All the other cases reacted with large, collisionally saturated rates, implying bond strengths >35 kcal mol^{-1}, except for the larger alkaline earths Sr^+ and Ba^+, whose noticeably slower rates were attributed to relatively lower bond strengths around 32 kcal mol^{-1}. Many of the $M^+(Cor)$ complexes reacted further to $M^+(Cor)_2$ with collisionally saturated rates, but several cases (Mg^+, Al^+, Si^+, In^+, Pb^+, Bi^+) reacted more slowly or not at all, indicating weaker bonds. The important role of transition-metal character in $M^+(Cor)_2$ bonding is suggested by the observation that transition metal ions (Sc^+ and Mn^+, for instance) rapidly formed $M^+(Cor)_2$ complexes, while comparable non-transition ions (Mg^+, Al^+, Si^+) did so poorly or not at all. The rates of formation of the various complexes were interpreted to estimate ion−neutral bond strengths, or at least to give upper or lower limits to the bond strengths. Atomic-ion/benzene bond strengths were generally well correlated in a qualitative way with the observed patterns of formation of ion/coronene complexes. Comparison with the isomeric ligand tribenzocyclyne (TBC) supports the interpretation that small ions (Ni^+, Cu^+) partially insert into the cavity of TBC, resulting in inhibited ML_2^+ formation relative to coronene.

Introduction

The binding of ions to π faces has considerable current interest, both in terms of the formation of ionic clusters and complexes in gas phase[1−4] and condensed phases, and also in terms of its participation in the folding and reactivity of proteins in solution.[5] The interaction of molecules with extensively conjugated π faces may also have interest related to interactions of ions with graphitic surfaces. It is thus useful to explore the complexation of gas-phase ions, such as atomic metal ions, with planar π systems of experimentally tractable size. Coronene is an excellent model system, being sufficiently large in conjugation to present a surface-like aspect to small ions, yet small enough for convenient detailed kinetic and thermodynamic investigation from a single-molecule point of view. It also provides comparisons and contrasts with binding to other π macrocycles like porphyrins, phthalocyanines, and cyclynes. The present study investigates the formation kinetics of monomer and dimer complexes of coronene with a variety of atomic ions (mostly metals). Analysis of the kinetics leads to conclusions about the binding energies and the favorable or unfavorable factors affecting complex formation, focussing particularly on the comparison with the isomeric molecule tribenzocyclyne (TBC) for which a similar body of data already exists.[3,4]

$C_{24}H_{12}$ macrocycles

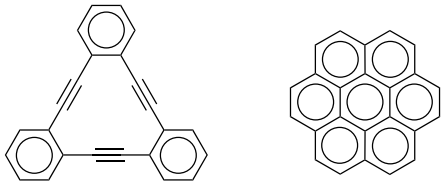

TBC coronene

When an atomic ion is trapped in the presence of a background pressure of coronene in the ion trap of the Fourier-transform ion cyclotron resonance (FT-ICR) spectrometer, the reaction sequence leading to ion/coronene complexes can be summarized as follows:

$$M^+ + Cor \underset{k_{a1}}{\overset{k_{ct1}}{\rightleftharpoons}} M^+(Cor) \underset{k_{a2}}{\overset{k_{ct2}}{\overset{Cor}{\rightleftharpoons}}} M^+(Cor)_2$$
$$M + Cor^+ \qquad M(Cor) + Cor^+ \qquad (1)$$

Cor represents the neutral coronene molecule, present at a pressure of the order of 10^{-8} Torr in the FT-ICR cell. As indicated in eq 1, charge transfer may potentially compete with complex formation both for the reaction of the bare metal ion and also for the reaction of the monomer complex. Such charge transfer reactions are often significant.

Under the low-pressure conditions used here, complex formation proceeds by the process of radiative association, in which the initial metastable collision complex is stabilized by emission of a photon.[6−8] In addition to giving a qualitative indication of favorable complex compositions, the kinetics of complex formation have been analyzed in a variety of cases to give values for complex binding energies (the RA, or radiative association, kinetics approach). Some previous investigations have studied the RA kinetics for reactions involving metal ions with benzene and other unsaturated hydrocarbons,[1,9−12] and there

* Author to whom correspondence should be addressed.

[⊗] Abstract published in *Advance ACS Abstracts,* October 1, 1997.

(1) Lin, C.-Y.; Dunbar, R. C. *Organometallics*. In press.

(2) Meyer, F.; Khan, F. A.; Armentrout, P. B. *J. Am. Chem. Soc.* **1995**, *117*, 9740.

(3) Dunbar, R. C.; Uechi, G. T.; Solooki, D.; Tessier, C. A.; Youngs, W.; Asamoto, B. *J. Am. Chem. Soc.* **1993**, *115*, 12477.

(4) Dunbar, R. C.; Solooki, D.; Tessier, C. A.; Youngs, W. J.; Asamoto, B. *Organometallics* **1991**, *10*, 52.

(5) Dougherty, D. A. *Science* **1996**, *271*, 163.

(6) Dunbar, R. C. Review: Ion-Molecule Radiative Association. In *Curr. Top. Ion Chem. Phys.* **1994**, *2*.

(7) Gerlich, D.; Horning, S. *Chem. Rev.* **1992**, *92*, 1509.

(8) Dunbar, R. C. *Int. J. Mass Spectrom. Ion Proc.* **1990**, *100*, 701.

(9) Ho, Y.-P.; Yang, Y.-C.; Klippenstein, S. J.; Dunbar, R. C. *J. Phys. Chem.* **1997**, *101*, 3338.

(10) Stöckigt, D.; Hrušák, J.; Schwarz, H. *Int. J. Mass Spectrom. Ion Proc.* **1994**, *149/150*, 1.

(11) Dunbar, R. C.; Uechi, G. T.; Asamoto, B. *J. Am. Chem. Soc.* **1994**, *116*, 2466.

S0002-7863(97)01625-9 CCC: $14.00

Table 1. Properties of the Atomic Ions Relevant to Complexation

ion	ΔIE^a	$k_{LO}{}^b$ ($M^+ + L$)	$k_{LO}{}^b$ ($ML^+ + L$)	cation valence config[c]	coord radius[d]	benzene bond energy[e]
Na	2.15	31	13	$2s^22p^6$ (^1S)	2.39[f]	28[g] (30[f])
K	2.95	25	11	$3s^23p^6$ (^1S)	2.84[f]	19[h] (15[f])
Rb	3.13	18	11	$4s^24p^6$ (^1S)	3.33,[i] 2.98[j]	(12[i])
Cs	3.40	15	11	$5s^25p^6$ (^1S)	3.19[j]	
Mg	−0.36	31	12	$3s^1$ (^2S)	2.32[k]	≤27[l] (30[k])
Sr	1.61	18	11	$5s^1$ (^2S)	3.17[i]	(17[i])
Ba	2.09	15	11	$6s^1$ (^2S)		
Al	1.30	29	12	$3s^2$ (^1S)	2.32[m]	35[n] (39[m])
Si	−0.86	29	12	$3s^23p^1$ (^2P)	2.50,[o] 2.25[p]	(32,[o] 44[p])
Sc[q]	0.74	23	11	$3d^14s^1$ (^3D)	2.30[r]	(40[r])
Ti[s]	0.47	23	11	$3d^24s^1$ (^4F)	2.06[r]	62[t] (61[r])
Cr	0.52	22	11	$3d^5$ (^6S)	2.11[r]	40[t] (37[r])
Mn	−0.14	22	11	$3d^54s^1$ (^7S)	2.30[r]	32[t] (35[r])
Fe[u]	−0.58	21	11	$3d^64s^1$ (^6D)	1.83[r]	49[t] (48[r])
Ni	−0.35	21	11	$3d^9$ (^2D)	1.75[r]	58[t] (59[r])
Cu	−0.44	20	11	$3d^{10}$ (^1S)	1.98,[i] 1.86[r]	52[t] (45,[i] 50[r])
Zn	−2.10	20	11	$3d^{10}4s^1$		
Y	1.07	18	11	$5s^2$ (^1S)	2.42[r]	(41[r])
Nb	0.41	17	11	$4d^4$ (^5D)	2.13[r]	64[v] (52[r])
Ag	−0.29	16	11	$4d^{10}$ (^1S)	2.35[r]	39[w] (37[r])
In	1.50	16	11	$4d^{10}5s^2$ (^1S)		
Te	−1.72	15	11	$5s^25p^3$ (^4S)		
Re	−0.47	13	11	$5d^56s^1$ (^7S)		
Pt	−1.32	13	11	$5d^9$ (^2D)		
Pb	−0.12	13	11	$6s^26p^1$ (^2P)		26[x]
Bi	0.00	13	11	$6s^26p^2$ (^3P)		≤36[y]

[a] Difference in ionization energy of the atom and coronene (positive values imply endothermic charge transfer from M^+ to coronene). IE of coronene = 7.29 (ref 31). [b] Langevin orbiting rate constant (10^{-10} cm^3 molecule^{-1} s^{-1}) assuming an isotropic polarizability of 38 Å^3 for coronene (according to ref 19). [c] References 32 and 33. [d] Ion-ring plane distance for benzene complexation (Å). [e] kcal mol^{-1}. Experimental numbers are given where available. Various *ab initio* calculated values are given in parentheses. [f] MP2/6-31G* (ref 34). [g] Reference 35. [h] Reference 36. [i] Present calculations, MP2/lanl2dz//MP2/lanl2dz. [j] Estimated by extrapolation from Na^+ using alkali crystal radii. [k] Reference 17. [l] Reference 37. [m] MP2/6-31G(d,p) (ref 10). [n] Reference 12. [o] Present calculations for C_{6v} symmetry, MP2/6-31G(d,p)//MP2/6-31G(d,p). Srinivas et al. (ref 24) obtained 34 kcal mol^{-1} binding for this structure with MP2/6-31G**//UHF/3-21G*. However, this complex is apparently not C_{6v}; see following footnote. [p] Srinivas et al. (ref 24) found this much stronger binding for an unsymmetrical π complex with the Si^+ considerably off center. [q] Sc^+ has a $3d^2$ (^3F) state lying 14 kcal mol^{-1} above the ground state that might possibly give more favorable bonding to π faces, but this possibility has not been pursued. [r] Reference 18. [s] Ti^+ has a $3d^3$ (^4D) state lying only 2 kcal mol^{-1} above the ground state, which is undoubtedly the state that complexes to π faces, and it is this state for which the binding energy and bond length are reported. [t] Reference 2. [u] Fe^+ has a low-spin state $3d^7$ (^4S) lying 6 kcal mol^{-1} above the ground state. This is probably the state that binds to π ligands. Bauschlicher's benzene calculations suggest that the more favorable binding of the low-spin configuration overcompensates for the atomic promotion energy by around 6 kcal mol^{-1}. The binding energy and bond length given here refer to this state. [v] Reference 38. [w] Reference 9. [x] Reference 39. [y] Reference 40.

have been some radiative association studies involving more complex ions reacting with aromatic molecules.[8,11,13−16]

An interesting point of comparison for the present work is a parallel study previously reported for the ligand tribenzocyclyne (TBC), which is a planar, highly conjugated isomer of coronene, but which has a central cavity potentially capable of accommodating a small atomic cation.[3,4] The metal ion/TBC results suggested that several small metal ions, most notably Ni^+ and Cu^+, inserted at least partially into the cavity, resulting in greatly suppressed formation of $ML_2{}^+$. It was, however, considered quite possible that this suppression of $ML_2{}^+$ was instead due to electronic effects in the metal−ligand binding, such as overfilling of the 18-electron shell. The comparison with coronene, which clearly has no cavity of possible importance, should be revealing in clarifying the role of cavity effects in forming these complexes, and differentiating the relative importance of cavity effects versus electronic effects.

For most of the elements +1 is an exotic oxidation state in condensed phases, and for the majority of elements no information about structural characteristics of their atomic monocation complexes is available from condensed-phase studies of stable complexes. In the course of considering the coronene and TBC complexes of atomic ions, we have been interested in the size of these ions in the context of π complexation. Theory gives the only feasible approach to assigning binding radii for most of the ions; fortunately a reasonable estimate of the bond length does not require a very large-scale calculation in most cases. The ion−ring distance in the benzene π complex can serve as a good measure of the π-complexation radius. For many first-row and a few second-row transition metal ions, the calculations of Bauschlicher's group give binding radii to benzene,[17,18] and various other values are available from the literature. A few additional calculations were carried out in the course of this work.

The set of atomic ions is shown in Table 1, along with several properties useful in thinking about the present results. For each ion the exothermicity (endothermicity) of charge transfer to coronene is given, along with the electronic configuration of the isolated-ion ground state. The association rates will be considered below relative to the calculated encounter rate

(12) Dunbar, R. C.; Klippenstein, S. J.; Hrusak, J.; Stöckigt, D.; Schwarz, H. *J. Am. Chem. Soc.* **1996**, *118*, 5277.
(13) Lin, Y.; Ridge, D. P.; Munson, B. *Org. Mass Spectrom.* **1991**, *26*, 550.
(14) Dunbar, R. C.; Faulk, J. D. *Chem. Phys. Lett.* **1993**, *214*, 5.
(15) Cheng, Y. W.; Dunbar, R. C. *J. Phys. Chem.* **1995**, *99*, 10802.
(16) Crestoni, M. E.; Fornarini, S. *Organometallics* **1996**, *15*, 5695.
(17) Bauschlicher, C. W. J.; Partridge, H. *Chem. Phys. Lett.* **1991**, *181*, 129.
(18) Bauschlicher, C. W. J.; Partridge, H.; Langhoff, S. R. *J. Phys. Chem.* **1992**, *96*, 3273.

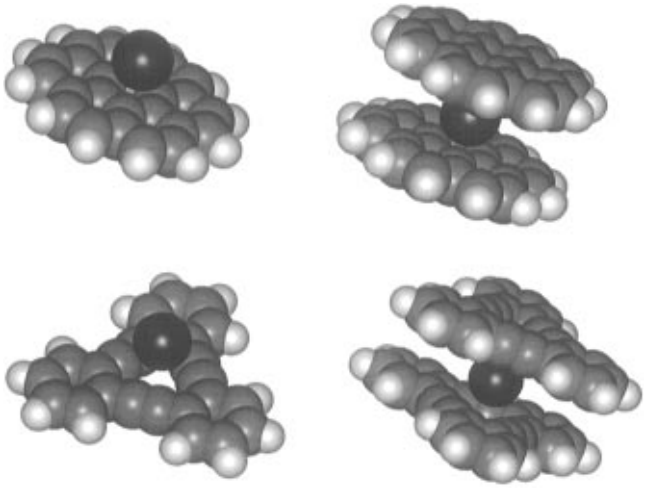

Figure 1. Models of ML and M^+L_2 complexes of coronene and TBC, illustrated for a metal ion with a ring/metal ion separation of 2.32 eV.

between the ion and the neutral: this is assumed to be the Langevin orbiting collision rate, based on the assumption that the long-range ion-induced dipole attractive force determines the encounter rate, and that coronene can be approximated for this purpose as having an isotropic polarizability of 38 A^3 (according to ref 19).

To illustrate these complexes, Figure 1 shows models of metal-ion complexes of coronene and TBC, using a complexation distance of 2.32 Å, and a displayed van der Waals radius for the metal ion of 1.40 Å (molecular mechanics MM2 force field structures for the hydrocarbons).

Experimental Section

The experiments were carried out in an electromagnet-based FT-ICR instrument used in previous laser desorption/ionization studies.[20,21] The ICR cell had 2.54 cm cubical geometry, in a magnetic field of 1.4 T. An IonSpec data system was used.

Atomic ions were produced by laser desorption/ionization from the solid element (or, in the case of Sr^+, from polycrystalline $SrCl_2$). The solid sample was mounted at the center of the trapping plate plane, so that the emerging ions traveled along the magnetic field lines into the center of the cell. A small prism mounted at the center of the opposite trapping plate deflected the incoming laser beam 90°, giving perpendicular laser incidence on the sample surface. The laser was focused onto the sample with an external lens of 20 cm focal length.

Coronene was introduced from a reservoir of powdered solid connected to the vacuum system. At the working temperature of 85 °C its volatility was sufficient to give a steady pressure of the order of 1×10^{-8} Torr. To have an unambiguous and reasonably homogeneous thermal environment for the cell, the entire high-vacuum can was maintained at 85 °C, as measured by a thermocouple mounted on the trapping plate.

No reliable absolute pressure measurement of coronene was available. To estimate the pressure and make an approximate assignment of the absolute rate constants, it was assumed that the fastest reaction observed proceeded at the Langevin orbiting collision rate. This fastest reaction turned out to be the charge transfer of non-thermalized iron ions, for which the theoretical orbiting collision rate constant is 21×10^{-10} cm^3 $molecule^{-1}$ s^{-1}. All the rates reported here are referenced to this assumed rate. This is a fairly crude calibration, both because it need not be true that the reference reaction proceeded on every collision as assumed and also because the collision rate of these iron ions, which were probably kinetically excited, might have been higher than the orbiting collision rate (due to hard-sphere collision effects). It seems reasonable to give a factor of 2 uncertainty to the absolute rate constants.

(19) Savchik, K. J.; Miller, J. A. *J. Am. Chem. Soc.* **1979**, *101*, 7206.
(20) Pozniak, B.; Dunbar, R. C. *J. Am. Chem. Soc.* **1994**, *116*, 4113.
(21) Pozniak, B.; Dunbar, R. C. *Int. J. Mass Spectrom. Ion Proc.* **1994**, *133*, 97.

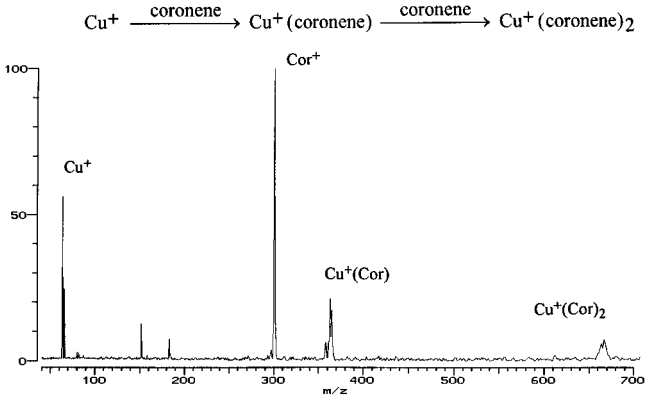

Figure 2. FT-ICR spectrum of the Cu^+/coronene system, at a reaction time of 2 s, showing the species participating in the kinetics of eq 1.

The pressure uncertainty is the dominant uncertainty in the rate constant calibrations, and since a pressure calibration error affects all the measurements equally, the relative rate constants across this data set are less uncertain. We would consider comparisons among these different rate constants to be accurate in general within 30%.

***Ab Initio* Calculations.** Useful computations are not yet available for the metal-ion/coronene system, nor for most benzene dimer complexes. However, calculations of the metal-ion/benzene monomer complexes give some insight into the π bonding. Some calculations were done here to complement the results available from the literature. The Gaussian 92 program suite[22] was used. For Si^+, Rb^+, Sr^+, and Cu^+ the structures were optimized and energies calculated at the MP2 level with the LANL2DZ basis set[23] in C_{6v} symmetry. For Si^+ a larger calculation was also made, with structure optimization in C_{6v} symmetry and energy calculation at the MP2 level with the 6-31G(d,p) basis set, allowing direct comparison with the similar calculation for Al^+,[10] although our Si^+ calculation was not a significant improvement on the calculation of Srinivas et al.,[24] which used nearly as high a computational level, and considered more geometries. Comparing different computational levels for Al^+ and Si^+, as well as for Cu^+, against Bauschlicher's calculations,[18] it appears that the insufficient flexibility of the LANL2DZ basis overestimates the metal-ring bond length by 0.1−0.2 Å, and underestimates the binding energy by perhaps 5 kcal mol^{-1}. However, counterpoise calculations suggest that basis set superposition error (BSSE) gives an offsetting overstimate of the binding energy by a few kilocalories per mole. Such small-basis, single-configuration calculations are thus substantially uncertain, but can provide a useful first indication of properties of the complexes.

Results

Atomic Ion Reactions. As a typical illustration, Figure 2 displays a mass spectrum corresponding to the reaction sequence of eq 1 for the Cu^+ case. By taking such spectra at various reaction times a time plot of the kinetics can be made and fitted to the kinetics of eq 1, as illustrated in Figure 3. Such fits produce the set of rate constants displayed in Table 2. We lack confidence in the Na^+ results: occasional laser shots yielded significant Na^+ peaks, for which no significant corresponding $Na(Cor)^+$ peaks were observed, indicating that complexation was slow. However, no systematic results for this ion were obtained, and uncertainty remains about this rate constant. Otherwise, the observations of the kinetics were satisfactory.

Metal Oxide and Hydroxide Ion Reactions. Sc^+, Y^+, Ti^+, and Nb^+ reacted with background water and/or oxygen, giving

(22) Frisch, M. J.; Trucks, G. W.; Schlegel, H. B.; Gill, P. M. W.; Johnson, B. G.; Wong, M. W.; Foresman, J. B.; Robb, M. A.; Head-Gordon, M.; Replogle, E. S.; Gomperts, R.; Andres, J. L.; Raghavachari, K.; Binkley, J. S.; Gonzalez, C.; Martin, R. L.; Fox, D. J.; Defrees, D. J.; Baker, J.; Stewart, J. J. P.; Pople, J. A., Gaussian 92/DFT; Gaussian, Inc.: Pittsburgh, PA, 1993.
(23) Hay, P. J.; Wadt, W. R. *J. Chem. Phys.* **1985**, *82*, 270.
(24) Srinivas, R.; Hrušák, J.; Sulzle, D.; Bohme, D. K.; Schwarz, H. *J. Am. Chem. Soc.* **1992**, *114*, 2802.

Table 2. Reaction Rate Constants and Efficiencies[a]

	reactions of M^+		reactions of ML^+		association efficiencies	
ion	k_{a1}	k_{ct1}	k_{a2}	k_{ct2}	Φ_{ra1} (Φ_{tot1})	Φ_{ra2} (Φ_{tot2})
Na^+	slow					
K^+	< 0.01	< 0.01			<0.001	
Rb^+	< 0.02	< 0.02			<0.001	
Cs^+	< 0.02	< 0.02			<0.001	
Mg^+	1.3	10.4	<1.0	<1.0	0.04 (0.38)	<0.1
Sr^+	2.5	0.0	2.8	0.0	0.11	0.25
Ba^+	2.5	0.0	4.8	0.0	0.10	0.44
Al^+	13.0	0.0	<0.1	<0.1	0.46	<0.01
Si^+	13.8	4.5	< 0.1	3.4	0.48 (0.64)	<0.01 (0.28)
Sc^+	5.8	0.0	3.2	0.0	0.25	0.29
Ti^+	6.3	0.0	4.6	0.0	0.28	0.43
Cr^+	6.6	1.1	3.8	0.0	0.30 (0.35)	0.34
Mn^+	8.9	0.0	3.5	1.4	0.40	0.31 (0.43)
Fe^+	6.0	6.0	6.0	9.0	0.29 (0.58)	0.55 (1.4)
Ni^+	2.5	3.8	3.8	0.0	0.13 (0.33)	0.34
Cu^+	3.1	3.5	4.5	0.0	0.16 (0.34)	0.41
Zn^+	< 0.2	6.4			<0.01 (0.32)	
Y^+	4.5	0.0	4.4	0.0	0.25	0.40
Nb^+	3.9	0.0	4.4	0.0	0.23	0.40
Ag^+	1.8	1.5	1.1	0.0	0.11 (0.20)	0.10
In^+	5.1	0.0	<0.1	<0.1	0.31	<0.04
Te^+	< 0.1	7.3			<0.01 (0.49)	
Re^+	1.4	3.0	5.6	0.0	0.10 (0.31)	0.51
Pt^+	0.25	4.5	3.8	0.0	0.02 (0.35)	0.34
Pb^+	1.4	3.5	< 0.1	1.9	0.10 (0.35)	<0.01 (0.17)
Bi^+	3.4	3.0	< 0.1	1.5	0.26 (0.49)	<0.01 (0.14)

[a] Association and charge transfer rate constants (10^{-10} cm^3 $molecule^{-1}$ s^{-1}). Φ_{ra} is the efficiency of radiative association per orbiting collision, using the Langevin orbiting rate for the collision rate constant. The sum of the association and charge transfer efficiencies is also given (Φ_{tot}) for the cases where the charge transfer reaction is significant.

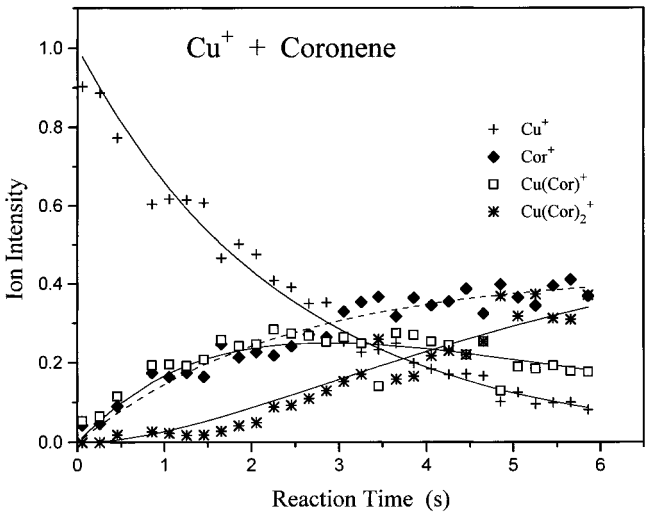

Figure 3. Time plot for the Cu^+/coronene system, showing the fit to the kinetics of eq 1 with use of the rate constants displayed in Table 2.

metal oxide ions (MO^+) and metal hydroxide ions ($M(OH)_2^+$). (The latter might have the form of hydrated oxides, rather than dihydroxides, which would be indistinguishable in these experiments, but we will write them in the dihydroxide form for convenience.) No further addition of oxygen-containing moieties beyond $M(OH)_2^+$ was observed.

These MO^+ and $M(OH)_2^+$ attached to coronene to form the $(Cor)MO^+$ and $(Cor)M(OH)_2^+$ species, with rates similar to the attachment rates of the corresponding bare metal ions. It was shown by ion-ejection studies that these same products ($(Cor)MO^+$ and $(Cor)M(OH)_2^+$) were also formed to some extent by reaction of $M(Cor)^+$ with background oxygen/water for these same four elements.

The $(Cor)MO^+$ ions attached a second coronene to form $(Cor)_2MO^+$, with rates which were somewhat slower (by about half) than the corresponding sandwich-formation rates for $(Cor)M^+$. The attachment of $(Cor)M(OH)_2^+$ ions to a second coronene to form $(Cor)_2M(OH)_2^+$ was either not observed or just marginally observable with very low rates.

Discussion

Nearly all atomic cations undoubtedly form inherently stable complexes with coronene, since the simple electrostatic attraction between the charge and the ligand is almost invariably greater than the thermal tendency for the complex to break up. Similarly, clustering of a second ligand onto the monomer complex probably always gives an inherently stable dimer complex. Accordingly experiments like the present ones do not address the question of inherent stability of the complexes, but rather the question of whether the complex is sufficiently strongly bound to give an observable extent of complexation on the experimental time scale (which requires that a complex be formed within a few hundred, or at worst a few thousand, ion-neutral collisions). Thus, although our goal is to gain insight into the binding energies of the complexes, the analysis and interpretation focus on the kinetics of complex formation.

Formation and Binding Energies of Monomer Complexes. Radiative association kinetics, as studied here, offer a particularly interesting application of such kinetic approaches to investigating binding energies, because the range of binding energies which turn out to be addressed by this approach covers the 20−50 kcal mol^{-1} region, which is typical of many metal−ligand bond strengths. Recent studies[12,25] have shown convincingly that in particular cases a detailed, quantitative analysis of

(25) Klippenstein, S. J.; Yang, Y.-C.; Ryzhov, V.; Dunbar, R. C. *J. Chem. Phys.* **1996**, *104*, 4502.

Table 3. Binding Energies (kcal mol^{-1}) Corresponding to Various Observed Collisional Efficiencies of Radiative Association in the Atomic Ion/Coronene System (Standard Hydrocarbon Model[27])

association product[a]	binding energy (kcal mol^{-1})		
	50%	10%	1%
ML^+	34	29	25
ML_2^+	40	34	29

[a] L is a hydrocarbon-type ligand the size of coronene, while M^+ is an atomic ion.

radiative association kinetics information, incorporating quantum chemical calculations and refined statistical kinetic theory, can lead to binding energy assignments with uncertainties of a few kilocalories per mole. For larger ligands like coronene, analysis at such a detailed level of theory is hard to achieve, but the less detailed generic approach that we have termed the "standard hydrocarbon" analysis[8,26,27] serves in a similar way to give binding energy estimates of useful precision with much more modest computational effort.

The standard hydrocarbon estimation, as described most recently in ref 27, gives estimates of ML^+ and ML_2^+ binding energies (for an ambient temperature of 350 K) as exemplified in Table 3. This suggests that an observed efficiency near collisional saturation corresponds to a bond strength $\gtrsim$35 kcal ($\gtrsim$40 kcal for ML_2^+); while a bond strength $\gtrsim$25 kcal ($\gtrsim$30 kcal for ML_2^+) is required to have a reasonable assurance of seeing association products at this temperature. These numbers delimit the range of bond strengths accessible to estimation by the RA kinetics approach for the coronene system.

The association efficiencies of the $M^+ + L$ reactions shown in Table 1 for many metals are in the range 25−50%; most of those that are lower than this appear to be partly or completely suppressed by competition with charge transfer such that the sum of $\Phi_a^{(1)}$ and $\Phi_{CT}^{(1)}$, which is designated Φ_{tot}, is of the order of 25 to 50%. Φ_{tot} values are given in parentheses in Table 2 for the ions where charge transfer is significant. Since so many of the systems are in this same highly efficient range, it seems likely that RA efficiencies in this range are essentially collisionally saturated, in the sense that after formation of the metastable complex, the complex either stabilizes or dissociates by exothermic charge transfer, and seldom or never redissociates to reactants. There are several reasonable explanations why collisionally saturated associations might not give 100% efficiencies in our measurements: First, the absolute pressure calibration could easily be wrong by a factor of 2; second, the encounter rates with coronene may be quite different from the calculated Langevin orbiting rates, which are based on idealized long-range forces and isotropic polarizability; third, every encounter may not result in a metastable collision complex, since it is easy to imagine that some collisions with the coronene molecule could result in the partners bouncing off without finding their way to the intimate complex configuration. To be conservative, we will consider that any case where the Table 2 efficiency Φ_{tot} is greater than 25% is likely to be collisionally saturated, and for such collisionally saturated cases we will assign an approximate lower limit to the binding energy. The following ions fall in this efficient, collisionally saturated set, for which we delimit the monomer complex binding energy as >32 kcal mol^{-1}: Al^+, Si^+, Sc^+, Ti^+, Cr^+, Mn^+, Fe^+, Ni^+, Cu^+, In^+, Re^+, Bi^+, and Pb^+. The following also appear likely to be collisionally saturated, but because of severe charge transfer competition, give less constrained upper limits: Mg^+ (>29 kcal mol^{-1}) and Pt^+ (>27 kcal mol^{-1}). Zn^+ and Te^+ show only charge transfer, and give no information about complexes. The alkali ions K^+, Rb^+, and Cs^+ (and probably Na^+) gave no observable complexes, limiting their binding energies to <22 kcal mol^{-1}. This leaves a small number of cases with low efficiencies (Sr^+, Ba^+, Y^+, Nb^+, Ag^+) for which we can compare the Table 2 efficiencies with the calculations illustrated in Table 3 to assign actual binding energies of about 32 kcal mol^{-1}. Comparing with the metal ion/benzene binding energies given in Table 1, it is seen that complex binding energies this large are not at all surprising, even for the closed-shell Al^+ case, and the experimental results on monomer formation mostly serve to confirm that metal ions bind to coronene at least as well as to benzene.

On the other hand, for the alkali ions, we conclude from these negative results that the ML^+ complexes with $M^+ = K^+$, Rb^+, and Cs^+ (and probably Na^+) are bonded by less than about 22 kcal mol^{-1}. As indicated in Table 1, K^+ binds to benzene by less than 20 kcal mol^{-1}, and Rb^+ is even weaker; so it is not surprising that binding to coronene is also weak. It seems likely that Na^+ will be found to associate with coronene at an observable rate, since it binds to benzene by 28−30 kcal mol^{-1} (Table 1), although the present results suggest that association with coronene is surprisingly slow.

The alkaline earths Sr^+ and Ba^+ also appear to be instances, though less dramatic than the alkalis, where association is signficantly slower than the collisional saturation rate. (Mg^+ also associates with fairly low efficiency, but in this case the large competing charge transfer rate obscures the interpretation.) Assuming that these association efficiencies reflect binding energy kinetic control, we can place the monomer binding energies for these two metals as 30−35 kcal mol^{-1}. This is somewhat greater than the calculated binding energies to benzene noted in Table 1, suggesting that these metal ions bind significantly better to coronene than to benzene.

Formation of Dimer (Sandwich) Complexes. A number of the ions form dimer complexes ML_2^+. Quite a few do so with efficiencies high enough to suggest collisional saturation, indicating binding energies higher than about 36 kcal mol^{-1}. Ions in this category include Ba^+, Sc^+, Ti^+, Cr^+, Mn^+, Fe^+, Ni^+, Cu^+, Y^+, Nb^+, Re^+, and Pt^+. Ions which do not form observable dimer complexes, limiting their binding energies to <32 kcal mol^{-1}, include Mg^+, Al^+, Si^+, In^+, Bi^+, and Pb^+. (Si^+ is a borderline case, since the fairly rapid charge transfer might suppress association entirely. However, it does not appear that the charge transfer k_{ct2} is collisionally saturated in this case, and on this basis we consider that sandwich formation is inherently slow for this ion.)

All of the first transition series form dimer complexes readily (except Zn^+, which is dominated by charge transfer), even the closed-shell Cu^+ ion. However, several small non-transition ions (Al^+, Si^+, Mg^+) do not. The limited data suggest a similar picture favoring transition metal complexation for the heavy ions, so that the transition metals Pt^+ and Re^+ form sandwiches readily, while the non-transition elements Bi^+ and Pb^+ do not. For the second-row metals, the same pattern almost holds true, with the transition element Nb^+ forming abundant sandwich complexes, while In^+ is less favorable. (Ag^+ is a borderline case where sandwich formation rate is substantial but apparently not quite collisionally saturated.) However, Y^+, a non-transition element, forms abundant sandwich complexes, which this simple-minded analysis does not account for.

The role of transition element character in stabilizing the ML_2^+ sandwiches is graphically shown in the contrast between first-row transition metals and comparable non-transition ions.

(26) Herbst, E.; Dunbar, R. C. *Mon. Not. R. Astron. Soc.* **1991**, *253*, 341.
(27) Dunbar, R. C. *Int. J. Mass Spectrom. Ion Proc.* **1997**, *160*, 1.

We can compare Sc^+ and Mn^+, for instance, with Al^+, Si^+, and Mg^+. Judging from the benzene complexation radii in Table 1, all of these ions have fairly similar radii, and one would expect the electrostatic binding contributions to be reasonably similar. However, it is observed that Sc^+ and Mn^+ form sandwich complexes near the collisional saturation rate, while none of the three non-transition ions gave an observable abundance of ML_2^+, which means that the former pair form dimer complexes which are 10 kcal or more stronger than the latter group.

The relatively higher propensity of the transition elements to form sandwich complexes might be rationalized by arguing that the presence of valence d electrons enhances sandwich binding for the transition elements, or alternatively that the presence of valence s or p electrons inhibits sandwich binding for the non-transition elements. Theoretical results[28] and experimental observations of the H_2O complexes of[29] Mg^+ and Al^+ have led Bauschlicher et al.[28] and Armentrout et al.[29,30] to a persuasive argument that it is the presence of outer s electrons in the non-transition elements that inhibits dimer complex formation. In this interpretation, the first ligand gains electrostatic binding energy by polarizing the s electron(s) away from the ligand, but the resulting polarization of the electron density around the metal ion reduces the electrostatic binding energy to a second ligand approaching from the other side. This is an attractive rationalization, but the alternative argument in terms of d-electron enhancement of transition metal sandwich bonding can certainly not be dismissed at our present level of understanding.

In speculating about the factors governing sandwich formation for the larger ions, we can draw from the limited evidence the suggestion that the ions containing metal ions with high ionization energies seem less likely to form dimer complexes; this might be expected on the basis of extensive charge shifting off of the metal ion in the monomer complex. The resulting more charge-delocalized monomer complex would have weaker electrostatic binding to the second ligand.

In terms of assigning binding energies to the sandwich complexes, the data of Table 2 pretty much divide into ions which form sandwiches readily, suggesting binding energies greater than about 35 kcal mol^{-1}, and those which do not form significant amounts of sandwich, suggesting binding energies less than about 30 kcal mol^{-1}. Except perhaps for Ag^+, there seem to be no cases of slow sandwich formation which could allow more precise assignment of binding energies.

Looking at the several small ions (Mg^+, Al^+, Si^+) whose rate of sandwich formation is low, it might be suspected that ring−ring repulsion plays a role in inhibiting formation of these complexes. However, a molecular modeling calculation (using the MMX force field in the PCMODEL package, Serena Software, Bloomington, IN) suggests that this is unlikely. The repulsion energy between two coronenes reaches 3 kcal mol^{-1} only at a separation of 3.6 Å, and is insignificant for separations much larger than this. Judging from the complexation radii in Table 1, none of these sandwich complexes would be likely to have such a small ring−ring separation, so ring−ring repulsions are unlikely to be significant. To the contrary, an attractive van der Waals potential well about 1.0 kcal mol^{-1} deep is predicted at a separation af about 4.4 Å, which could conceivably play a minor role in sandwich stabilization for small ions.

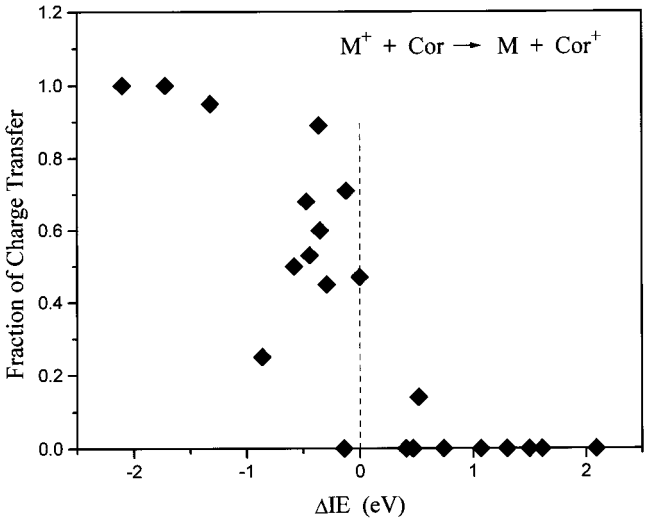

Figure 4. Charge transfer rate from Table 2 as a fraction of total reaction rate, plotted against the electron transfer endothermicity.

Comparison of Coronene and TBC. Comparing the present coronene results for Ni^+ and Cu^+ (and Fe^+ to a lesser extent) with the corresponding results for TBC[3,4] gives convincing support to the importance of cavity effects in the TBC case. While ML_2^+ formation was severely depressed for these two ions in the TBC case, it is seen in Table 2 that ML_2^+ formation is very efficient in the coronene case. It is most natural to infer that it is the partial or complete accommodation of the metal ion in the TBC cavity in $M(TBC)^+$ that leads to this contrasting behavior. This comparison makes a very strong case that it is in fact the cavity effect, and not any electronic effects, that is responsible for the suppressed ML_2^+ formation for first-row late transition metals reacting with TBC.

The other notable contrast between TBC and coronene is the failure of the latter to associate with K^+ and Na^+, while the K^+(TBC) and Na^+(TBC) complexes were readily formed. K^+ is much too large to penetrate into the TBC cavity, and the reason for this contrasting behavior is not clear. Cs^+ did not associate with either macrocycle, which is not surprising on the basis of its large size and weak electrostatic binding.

Charge Transfer Reactions. Charge transfer from M^+ to coronene often happens in competition with, or to the exclusion of, association. The degree of correlation between charge transfer rates and exothermicities is shown graphically in Figure 4 as a plot of the fractional charge transfer versus ΔIE. The charge transfer probability is low for endothermic cases, and generally rises with increasing exothermicity. (The non-zero rate for Cr^+, whose charge transfer is 0.45 eV endothermic, is surprising, and probably reflects the persistence of a long-lived excited state in the Cr^+ population.) However, the quantitative trend is ragged, and there is nothing close to a smooth rise in electron transfer probability with increasing exothermicity. A

(28) Bauschlicher, C. W. J.; Partridge, H. *J. Phys. Chem.* **1991**, *95*, 9694. Bauschlicher, C. W. J.; Sodupe, M.; Partridge, H. *J. Chem. Phys.* **1992**, *96*, 4453.
(29) Dalleska, N. F.; Tjelta, B. L.; Armentrout, P. B. *J. Phys. Chem.* **1994**, *98*, 4191.
(30) Armentrout, P. B. *Acc. Chem. Res.* **1995**, *28*, 430.
(31) Lias, S. G.; Bartmess, J. E.; Liebman, J. F.; Holmes, J. L.; Levin, R. D.; Mullard, W. G. *J. Phys. Chem. Ref. Data* **1988**, *17*, *Suppl. 1*.
(32) Rosi *J. Phys. Chem.* **1990**, *94*, 8658.
(33) Moore, C. E. *Atomic Energy Levels as Derived from the Analyses of Optical Spectra*; National Bureau of Standards: Washington, DC, 1971; Vol. NSRDS-NBS 35.
(34) Caldwell, J. W.; Kollman, P. A. *J. Am. Chem. Soc.* **1995**, *117*, 4177.
(35) Guo, B. C.; Purnell, J. W.; Castleman, A. W. J. *Chem. Phys. Lett.* **1990**, *168*, 155.
(36) Sunner, J.; Nishizawa, K.; Kebarle, P. *J. Phys. Chem.* **1981**, *85*, 1814.
(37) Willey, K. F.; Yeh, C. S.; Robbins, D. L.; Duncan, M. A. *J. Phys. Chem.* **1992**, *96*, 9106.
(38) Buckner, S. W.; Freiser, B. S. *J. Phys. Chem.* **1989**, *93*, 3667.
(39) Stanley, R. J.; Castleman, A. W. J. *J. Chem. Phys.* **1990**, *92*, 5770.
(40) Willey, K. F.; Cheng, P. Y.; Duncan, M. A. *J. Am. Chem. Soc.* **1991**, *113*, 4721.

good correlation would not really be expected for this plot, since the probability of charge transfer depends on the competition between charge transfer and association, and thus should be a function of binding energy as well as ΔIE. Thus, for instance, Pb^+ and Bi^+ have relatively high charge transfer probabilities, but this likely reflects in part weak binding to these large ions, disfavoring the association channel. However, further analysis is futile in the absence of good knowledge of the binding energies.

Correlation with Ion/Benzene Binding Energies. The binding energies given in Table 1 for binding of a number of atomic ions to benzene are interesting as an indication of the strength of binding to π faces. With its larger polarizability coronene should form somewhat stronger electrostatic complexes than benzene, but comparable behavior might be expected. It is unsurprising that K^+ and Rb^+ do not give observable coronene complexes, since Table 1 suggests that, even allowing for a binding energy increase for coronene, their binding energies are unlikely to exceed the $\sim$25 kcal mol^{-1} that would be required. It is less clear why Na^+ should be slow. Sr^+ is the other interesting ion for which a rather low binding energy is predicted, and rather slow association is observed. However, this point of view fails to account for the rapid sandwich formation by Sr^+; this case clearly needs further consideration. None of the other ions in Table 1 has a low enough predicted binding energy that one would expect association to form the monomer complex to be slow.

Conclusions

With the exception of the alkali ions and a few ions where charge transfer dominates the chemistry, all of the atomic ions studied form complexes with coronene of sufficient strength to be observed readily under radiative association conditions. Only for a few cases (Mg^+, Ba^+) does the complex appear to be weak enough to reduce the radiative association rate significantly below the encounter rate. Sandwich formation is observed more selectively. Several ions have sandwich formation rates unobservably slow, or at least clearly slower than the encounter rate (Mg^+, Al^+, Si^+, In^+, Pb^+, Bi^+).

For sandwich complex formation the role of valence d electrons is vividly shown by the comparison of the nontransition ions Al^+, Si^+, and Mg^+, which form sandwiches poorly if at all, and comparable transition metal ions like Sc^+ and Mn^+, which form sandwich complexes abundantly. The limited number of examples among heavier elements provide some support for a similar role transition-metal character in enhancing sandwich complex formation, but the evidence for this generalization is rather thin.

A particularly interesting contrast exists between the cavity-containing TBC molecule and the cavity-free coronene case. Small ions, particularly Ni^+ and Cu^+, appear to insert at least partially into the TBC cavity to a sufficient extent that sandwich formation is severely inhibited, while with coronene these ions form sandwiches at collisionally saturated rates.

Acknowledgment. The support of the donors of the Petroleum Research Fund, administered by the American Chemical Society, and of the National Science Foundation, is gratefully acknowledged. We thank Prof. Peter Armentrout for informative discussions of sandwich-complex binding.

JA9716259